Pure Appl. Chem., Vol. 71, No. 11, pp. 2085–2094, 1999.
Printed in Great Britain.

Electroluminescent properties of functional π-electron molecular systems*

Zakya H. Kafafi[1,†], Hideyuki Murata[1], Lisa C. Picciolo[1], Hedi Mattoussi[1], Charles D. Merritt[1], Yasuhiro Iizumi[2] and Junji Kido[2]

[1]*US Naval Research Laboratory, Washington DC 20375, USA*
[2]*Graduate School of Engineering, Yamagata University, Yamagata 992, Japan*

Abstract: Molecules with delocalized π-electrons possess attractive electroluminescent properties, and have been recently incorporated as the active emissive layers in organic light-emitting devices. In particular, electroluminescent molecular composites using a highly fluorescent guest, with/without carrier trapping properties, and a host with dual luminescent and carrier transport properties are the focus of this study. Devices based on these luminescent functional π-electron molecular systems exhibited high electroluminescence quantum efficiency, and good thermal and temporal stability, with ease of color tunability. The paper discusses the mechanisms of light-emission that lead to superior performance in these molecular devices. Efficient Förster energy transfer from the host to the guest molecules, and direct carrier recombination at the highly fluorescent guest molecules are proposed as the two mechanisms responsible for high efficiency.

INTRODUCTION

In the last decade, the electroluminescent properties of functional π-electron molecular and polymeric systems have been the subject of numerous studies [1–12]. These materials have been used as the active emissive layers in organic light-emitting diodes. Various techniques have been used to enhance the electroluminescence (EL) quantum efficiency, and improve the color tunability. One effective approach has been the use of selective molecular doping of organic solid thin films with highly fluorescent guest molecules, e.g. laser dyes [6,8–12]. This method takes advantage of the large fluorescence quantum yield (close to unity in some cases) of the guest molecule and reduces the degree of exciton quenching, often observed in neat solid films. High photoluminescence (PL) quantum yields are thus achievable in composite films via efficient Förster energy transfer from host to guest molecules [13]. In the case of EL, the exciton is created upon electron and hole recombination on the host molecule, and is followed by rapid energy transfer to the guest molecule via long-range (3–10 nm) dipole-dipole coupling (Förster mechanism). Energy transfer may also occur by electron exchange between neighboring molecules resulting in diffusion of excitons. This is known as Dexter energy transfer and does not require the conservation of spins [14]. Electron and hole recombination can also take place directly on the guest molecule, which may serve as a trap and/or a hopping site for the carrier of interest.

Molecularly doped organic semiconductors, which exhibit very high fluorescence quantum yields in the solid state [15,16], have been recently developed at the Naval Research Laboratory (NRL). Absolute PL quantum efficiency close to unity has been achieved for some of these molecularly doped films. Detailed analysis of the data yields strong evidence for Förster dipole-dipole interaction between the

* Lecture presented at the 4th International Symposium on Functional Dyes—Science and Technology of π-Electron Systems, Osaka, Japan, 31 May–4 June 1999, pp. 2009–2160.
† *Corresponding author*: E-mail: kakafi@ccf.nrl.navy.mil

guest and the host molecules as the principal mechanism for efficient energy transfer [17]. An energy transfer rate of a nanosecond was obtained with a transfer range on the order of 3–4 nm. These highly luminescent molecularly doped organic semiconductors were employed as the active emissive layers in molecular organic light-emitting diodes (MOLEDs) [8–11,18,19]. Devices based on multilayered structures using these active emissive layers are highly efficient. In addition, they are thermally and temporally stable [18,19]. For instance, stable device performance up to 90 °C was demonstrated using tris-(8-hydroxyquinolinato) aluminum (III) doped with N,N′-diethylquinacridone as the active emissive layer, and thermally stable hole injection and transport layers [18]. In addition, the power conversion efficiency improves as a function of increasing temperature. For instance, the luminous power efficiency increases from 4.6 *lm*/W at room temperature to 7.5 *lm*/W at 90 °C at 100 cd/m^2. The durability of these devices has been evaluated at room and high temperatures at constant DC current. The half-decay time of the initial luminance (850 cd/m^2) of the device, measured at 10 mA/cm^2, is 200 h at 80 °C. When measured at room temperature, the half-life is extended to 3200 h.

The paper reviews the mechanisms of light-emission that lead to superior performance in these molecular devices. Efficient Förster energy transfer from the host to the guest molecules, and direct carrier recombination at the highly fluorescent guest molecules are proposed as two possible mechanisms [8–10].

EXPERIMENTAL SECTION

Figure 1 depicts the device configuration and the chemical structures of the hole and electron transporters as well as the fluorescent guest molecules used in this study. N,N′-diphenyl-N,N′-bis(3-methylphenyl)-1,-biphenyl-4,4′-diamine (TPD) is used as the host and/or hole transporter. Tris-(8-hydroxyquinolinato) aluminum (III) (Alq_3) or tris-(8-hydroxyquinolinato) gallium (III) (Gaq_3) or tris-(4-methyl-8-hydroxyquinolinato) aluminum (III) ($Almq_3$) serves the role of a host and/or electron transporter. N,N′-diethylquinacridone (DEQ) and 5,6,11,12-tetraphenylnaphthacene (rubrene) are the fluorescent guest molecules. TPD was obtained from H.W. Sands Corp.; Alq_3 and rubrene were purchased from TCI America and Aldrich Chemicals Co., respectively. DEQ was synthesized from quinacridone (from TCI America Ltd) and iodoethane by use of a base and a phase transfer catalyst [8]. $Almq_3$ was prepared by reacting aluminum chloride hexahydrate and 4-methyl-8-hydroxyquinone [20]. Gaq_3 was synthesized from 8-hydroxyquinoline and gallium chloride ($GaCl_3$) both purchased from Aldrich Chemical Co. [21]. All materials were purified by vacuum train sublimation prior to use.

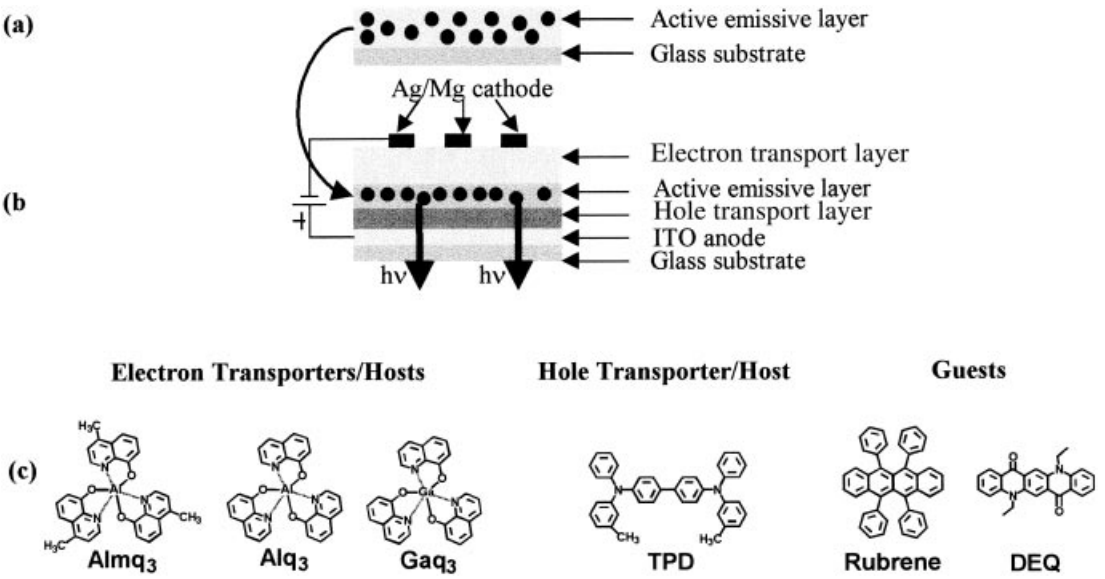

Fig. 1 (a) Configuration for PL study of the active emissive layer. (b) Device structure. (c) Molecular structures of the materials used in this study.

Films of neat and molecular composites used for spectroscopic characterization are prepared, as single structures on SiO_2 glass substrates (see Fig. 1a), by high vacuum vapor deposition (background pressure $\approx 1 \times 10^{-7}$ Torr). The film thickness is controlled by fixing the rate and time of deposition, and is measured by ellipsometry. The rate of deposition is monitored using a quartz crystal microbalance, with nanogram sensitivity. *Ex-situ* UV-Vis absorption and *in-situ* PL spectra are collected using a Perkin-Elmer Lambda 9 Spectrophotometer, and the 325 nm line from a He-Cd laser as the excitation source and a spectrograph equipped with a CCD detector, respectively. Measurements of the absolute photoluminescence quantum yield, ϕ_{pl}, are carried out in an inert (dry N_2) atmosphere, using an integrating sphere (from Labsphere Inc.) [15].

Details on device fabrication have been described elsewhere [9,10]. Briefly, devices (see Fig. 1b) are prepared on ITO patterned glass substrates by subsequent vapor deposition (below 10^{-7} Torr) of several organic layers. A film of Mg:Ag (12:1 by weight) alloy is prepared by codeposition of Mg and Ag through a shadow mask on top of the organic layers. The total thickness of the organic layers, similar to that of the Mg:Ag film, is on the order of 100 nm. The substrate holds four active emitting areas, each is $2\,\text{mm} \times 2\,\text{mm}$. Electroluminescence (EL) spectra are recorded using optical fibers that guide the light from within a glove box filled with dry nitrogen where the device is held and to an external spectrograph. Current density-voltage-luminance measurements are conducted using a Keithley 238 high-current source measurement unit and a Minolta LS-110 luminance meter.

RESULTS AND DISCUSSION

Photoluminescence of the active emissive layer

Figure 2 shows a comparison between the extinction coefficient spectra of rubrene and DEQ, and the normalized PL spectra of neat films of the various hosts: TPD, Alq_3, Gaq_3, and $Almq_3$. A strong spectral overlap is observed between the absorbance of the guest molecule and the emission of the hosts Alq_3, Gaq_3, and $Almq_3$, respectively. In the case of TPD, the spectral overlap does not appear to be as large as with the metal chelates. Good spectral overlap of the guest absorbance and the host PL is necessary for efficient Förster energy transfer from host to guest molecules [15].

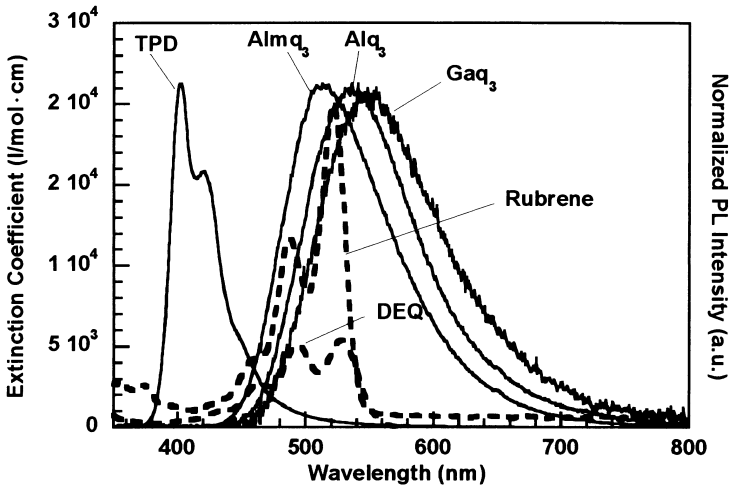

Fig. 2 Absorption spectra of guests (rubrene and DEQ) versus PL spectra of hosts (TPD, $Almq_3$, Alq_3, and Gaq_3).

Figure 3 shows the PL spectra of films of DEQ:$Almq_3$ composites which are displayed as a function of guest molecule concentration. Fluorescence of the composite films originates almost entirely from the guest molecules. Weak contribution from the host ($\approx$12–15%) is observed at a guest concentration below $\approx$0.4 mol%, but decreases rapidly to <2% at higher DEQ concentrations (>1 mol%). These results indicate that UV excitation of the host molecules primarily occurs and is followed by rapid and efficient energy transfer ('down conversion') from the excited host to the dispersed guest molecules in the host

matrix. Hence Förster dipole-dipole interaction between the guest and the host molecules is proposed as the principal mechanism for this energy transfer. This Förster energy transfer appears to be faster and more efficient than other competing processes, e.g. direct radiative and non-radiative decays of the host excitons. This mechanism has been further verified by time-resolved photoluminescence: an energy transfer rate on the order of a nanosecond was obtained with a transfer range of 3–4 nm [17]. This fast and efficient energy transfer combined with highly fluorescent guest molecules results in molecular composites with very high PL quantum yields approaching the maximum value of unity in some cases.

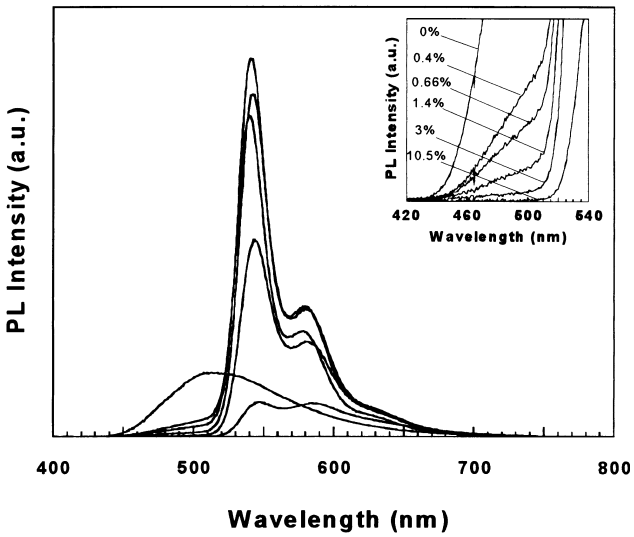

Fig. 3 PL spectra of DEQ:$Almq_3$ composite films as a function of DEQ concentration ranging from 0 mol% to 10.5 mol%.

The absolute photoluminescence quantum yields (ϕ_{pl}) have been measured for the neat and composite films. Figure 4 shows the dependence of the ϕ_{pl} on the concentration of the guest material. The absolute ϕ_{pl} of pure Gaq_3, Alq_3, and $Almq_3$ are 0.13, 0.25 and 0.42, respectively. TPD has $\phi_{pl} = 0.35$. Upon doping with DEQ or rubrene, the PL quantum yield increases as the concentration of the guest molecule is increased until it reaches its maximum value at an optimum dopant concentration. The absolute PL quantum yield of all of the rubrene-doped metal quinolate films reach ≈1.0 at a guest concentration of ≈1.0 mol%. Further doping leads to self-quenching of the fluorescence due to increased interactions between the guest molecules.

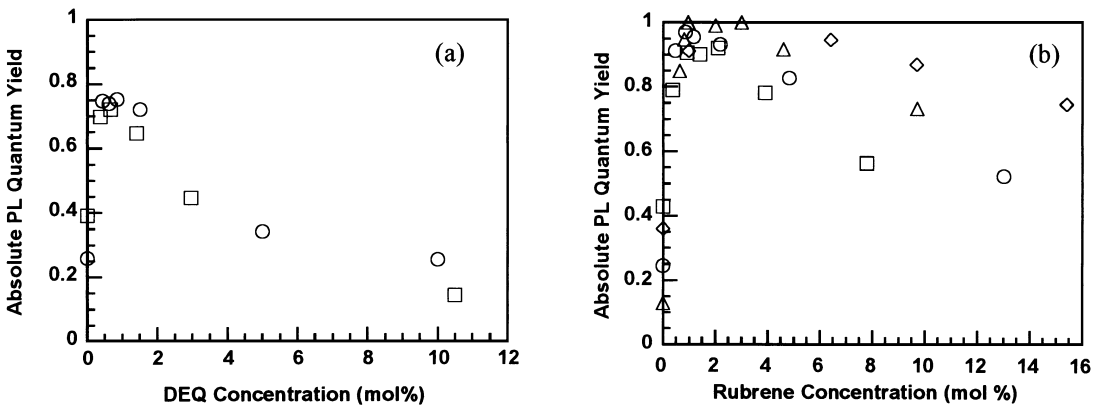

Fig. 4 Absolute PL quantum yield of composite films as a function of guest molecule concentration. (a) Alq_3 (circles) and $Almq_3$ (squares) films are doped with DEQ. (b) Alq_3 (circles), $Almq_3$ (squares), Gaq_3 (triangles), and TPD (diamonds) films are doped with rubrene.

Neither the PL quantum yield of the host nor the *extent* of the spectral overlap between the two guests and the four hosts used in this study appear to affect the maximum achievable ϕ_{pl} of these composite films. The maximum ϕ_{pl} of the composite films appears to be primarily determined by the molecular ϕ_{pl} of the guest molecule, and is very close to the value measured in dilute liquid solutions of the guest molecules [ϕ_{pl} (rubrene) = 1; ϕ_{pl} (DEQ) = 0.75]. Hence, the maximum achievable solid state fluorescence quantum yield of molecular composite films is the same as the ϕ_{pl} of the guest molecule. This result suggests that the guest molecules are well dispersed in the host matrices, and efficient energy transfer from host to guest, close to 100%, has been achieved. This good energy transfer is observed in spite of the differences in the magnitude of the spectral overlaps measured for each guest and the different hosts used in the study. For instance, the amount of spectral overlap, referred to as the overlap integral, was calculated for rubrene and each of the host materials [15]. The overlap integrals, calculated relative to Alq_3, are 0.7 and 1.2 for Gaq_3 and $Almq_3$, respectively [21]. A factor of 3.5 was measured for the ratio of the overlap integrals of rubrene: Alq_3 and rubrene: TPD composite films at their optimum dopant concentration [15].

Electroluminescence of the active emissive layer

Figure 5 shows the external EL quantum efficiency (η_{el}) for the active emissive layer incorporated in a multilayered device as a function of dopant concentration. The active layers consist of DEQ doped into Alq_3 or $Almq_3$, or rubrene doped into Alq_3 or Gaq_3 or $Almq_3$ or TPD, respectively. An enhancement in the η_{el} is observed when the active layer is doped with either DEQ or rubrene. At a first glance, the dopant concentration dependence of the EL and PL efficiencies appear to be quite similar increasing at low concentrations of DEQ or rubrene, reaching a maximum then falling off at high concentrations presumably due to aggregation quenching. A closer look, however, shows that the maximum η_{el} achieved when the active layer consists of either DEQ or rubrene in the host $Almq_3$ is much larger than that observed in all the other hosts. In particular, if one compares the maximum η_{el} in all the metal quinolate-based devices when rubrene is used as the dopant, a maximum η_{el} of ≈2.2% is achieved when the host is Gaq_3 or Alq_3 whereas a much higher η_{el} of 2.9% is reached when $Almq_3$ is the host. A similar effect is observed when DEQ is used as the guest molecule. This result is in contrast to the PL quantum yield concentration dependence when in all cases the maximum ϕ_{pl} achieved was the same for all hosts and was only a function of the guest molecule used. The radiative decay processes of the singlet exciton in photoluminescence and electroluminescence should be similar, assuming no interaction between the excited state of the host and the charge carriers. Assuming that the same number of host excitons are created by carrier recombination, one would expect that the maximum EL quantum efficiency will not change for the same dopant irregardless of the host matrix. Evidently, this is not the case. Differences in the maximum value for the EL efficiencies measured in different hosts may be attributed to differences in the creation efficiency of host excitons due to the carrier transport properties of the host matrices.

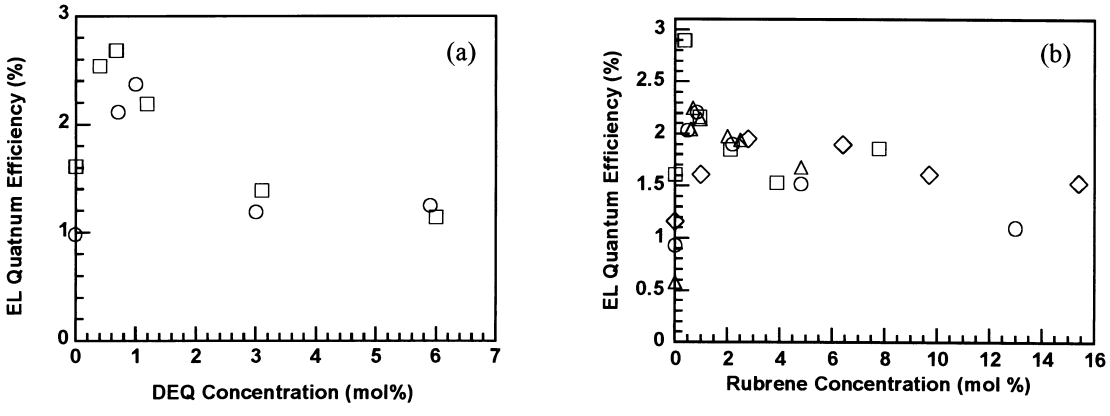

Fig. 5 External EL quantum efficiency of devices as a function of guest molecule concentration in the emissive active layer. (a) The active emissive layer is Alq_3 (circles) or $Almq_3$ (squares) doped with DEQ. (b) The active emissive layer is Alq_3 (circles) or $Almq_3$ (squares) or Gaq_3 (triangles) or TPD (diamonds) doped with rubrene.

Figure 6a shows the EL spectra of the devices, using films of $Almq_3$ doped with DEQ, as a function of dopant concentration. The EL and PL spectra (Fig. 3) are very similar, and show light emission primarily from DEQ with a small contribution from the host. However, the contribution of $Almq_3$ seems to persist in the EL spectra even at relatively high dopant concentrations. This is in contrast with the PL spectra (see Fig. 3), where no emission from $Almq_3$ is observed at high DEQ concentrations due to the efficient Förster energy transfer from $Almq_3$ to DEQ. Figure 6b gives the EL spectra of the device as a function of the thickness of the DEQ-doped $Almq_3$ layer. Contributions from $Almq_3$ are seen and continue to decrease as the thickness of the doped region increases up to 53 nm. A minimum thickness of 55 nm or larger seems to be necessary to totally eliminate emission from the adjacent undoped $Almq_3$ layer. This width is much larger than that of devices using DEQ-doped Alq_3 as the active emissive layer, where a thickness of 35 nm was found to be sufficient to totally eliminate contributions from the adjacent electron transport layer. The residual EL emission from $Almq_3$ can be ascribed to a mismatch between the doped region and the carrier recombination zone in $Almq_3$ as depicted in Fig. 7. If the carrier recombination zone is wider than the width of the DEQ-doped $Almq_3$ layer, some of the $Almq_3$ excitons, which are created outside the energy transfer radius, can radiatively decay and contribute to the EL spectra.

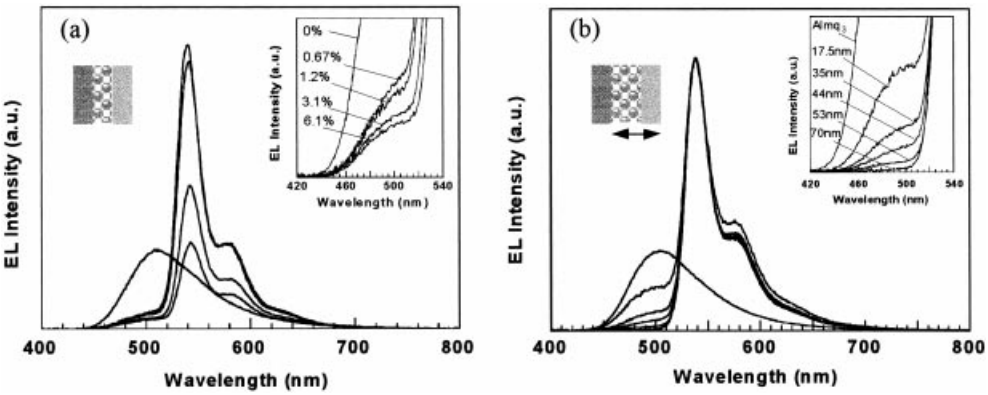

Fig. 6 EL spectra of $Almq_3$ doped with DEQ as a function of (a) DEQ concentration ranging from 0 mol% to 6.1 mol% and (b) thickness at doped region ranging from 17.5 nm to 70 nm.

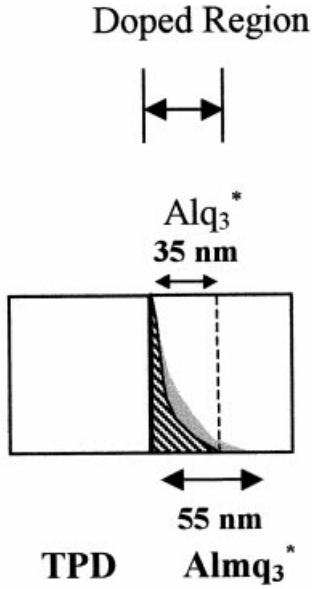

Fig. 7 Carrier recombination zone versus doped region in devices where the active emissive layer is doped Alq_3 or doped $Almq_3$.

Electroluminescence mechanism in MOLEDs where the active emissive layer is rubrene doped into TPD

Rubrene has been shown to be a very effective guest in the hole transporter TPD giving rise to devices with good efficiency and durability [9,10,22]. Experiments have been undertaken to determine the electron-hole recombination region and delineate the EL mechanism that gives rise to such good device performance. Since the emission is primarily from rubrene, carrier recombination has to occur inside TPD and/or inside Alq_3 near the TPD/Alq_3 interface. EL emission in single-layered devices composed of either undoped or doped TPD with rubrene has been observed [10]. This is direct evidence that electrons can be directly injected into TPD, previously known as an electron blocker, at the TPD/Alq_3 interface. Since very high PL quantum yield, close to unity, has been measured in rubrene-doped TPD films which indicates efficient energy transfer from TPD to rubrene [15], a similar process may also occur in electroluminescence. If electrons and holes primarily recombine inside the electron transport layer Alq_3, energy transfer from Alq_3 to rubrene can take place [15]. In addition, direct electron-hole recombination on rubrene molecules is another possibility since rubrene has been shown to act as a shallow hole trap in TPD. One can distinguish between these EL mechanisms by comparing the spatial relationship of the emission region and the recombination zone in the active emissive layer. If direct carrier recombination on the guest is the dominant mechanism, the recombination and emission zones should be identical. On the other hand, if energy transfer from Alq_3 to rubrene is the dominant mechanism, it would occur near the TPD/Alq_3 interface within the Förster energy transfer range from Alq_3 to rubrene. In the case of energy transfer from TPD to rubrene, the emission zone would be within the diffusion length of the TPD singlet excitons, and would be greater than that of the recombination zone dictated by the electron penetration depth in TPD.

The sum of the diffusion length of TPD excitons and the penetration depth of electrons into TPD, can be determined by using a doped layer as the sensing layer. Within the undoped TPD layer, a rubrene-doped TPD layer with 5 nm thickness was inserted. Figure 8 shows the EL quantum efficiency of these multilayered devices and their EL spectra as a function of the spacer thickness (undoped TPD), distance of the sensing layer from the TPD/Alq_3 interface. Changing the spacer thickness significantly affects the EL quantum efficiency as well as the EL spectra. By increasing the spacer thickness to 5 nm, the quantum efficiency is quickly reduced and approaches the value of that of the control device where the active layer consists of undoped Alq_3. As shown in Fig. 8b, increasing the spacer thickness above 5 nm nullifies the contribution from rubrene in the EL spectra and leads to that characteristic of Alq_3. These results suggest that the sum of the diffusion length of TPD excitons and the penetration depth of electrons into TPD, cannot be greater than 5 nm from the TPD/Alq_3 interface in the control device. On the other hand, energy transfer from Alq_3 to rubrene can only take place via dipole-dipole interaction using the Förster formalism. The energy transfer range is on the order of 3–4 nm [17], and energy transfer from either TPD or Alq_3 to rubrene would be also limited to this distance. Figure 9 shows the external EL quantum efficiency of several devices as a function of the thickness of the rubrene-doped TPD layer. The primary enhancement in the efficiency occurs within a 5 nm thick region from the TPD/Alq_3 interface. However, the EL efficiency continues to increase up to a doped layer thickness of 20 nm and remains essentially constant going from 20 to 50 nm. These results indicate that the width of the emission zone in the rubrene-doped TPD active emissive layer is about 20 nm. This wide emission zone cannot be explained solely by an EL mechanism that involves energy transfer from TPD or Alq_3 to rubrene, which would have limited the emission depth to 5 nm. Direct electron-hole recombination on rubrene is a plausible EL mechanism that can explain this wide emission zone of 20 nm. However, this may require that rubrene doping may have extended the electron penetration depth into TPD beyond 5 nm, i.e. an enhancement in electron mobility. The increase of electron mobility by rubrene doping has been directly confirmed by drift mobility measurements in rubrene-doped TPD films [23]. Since rubrene is expected to have an electron affinity much higher than TPD, the increase of electron mobility by rubrene doping can be attributed to the creation of a new electron hopping site on rubrene [23].

Figure 10 depicts the electroluminescence spectra as a function of rubrene concentration, which indicates that emission, is primarily from rubrene. However, there is a considerable contribution from the adjacent Alq_3 layer, which diminishes, as the concentration of rubrene is increased but never totally disappears. This result indicates that, in addition to direct carrier recombination on rubrene, electron and

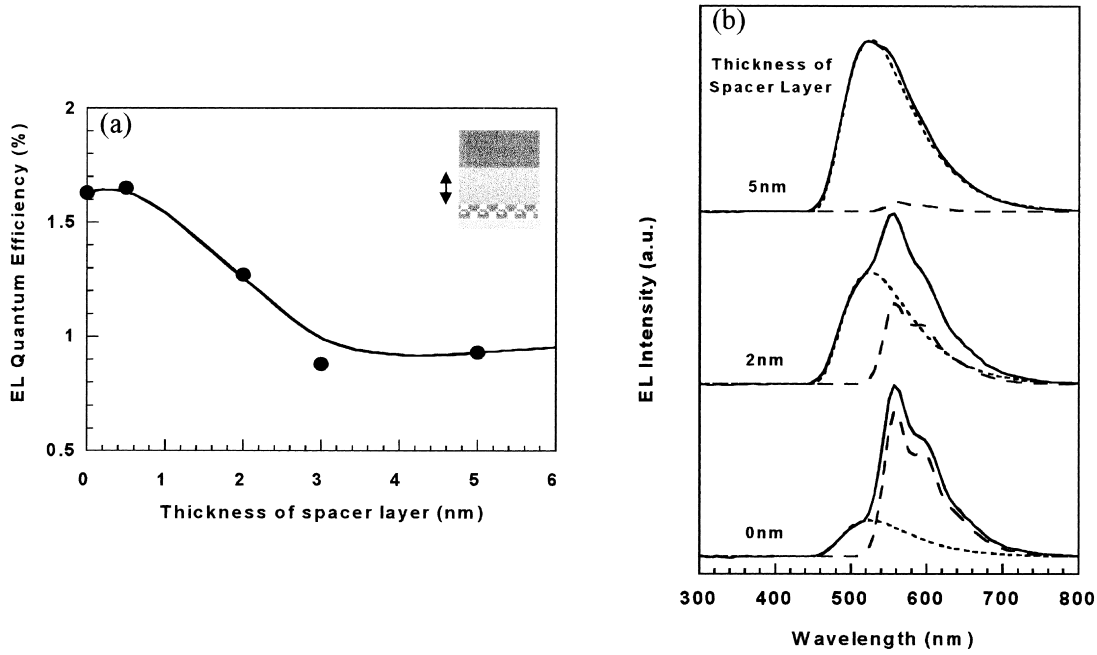

Fig. 8 (a) EL quantum efficiency and (b) spectra as a function of the thickness of the spacer layer (undoped TPD). The EL spectra (solid line) has been deconvoluted to those of rubrene (broken line) and Alq_3 (dotted line). The sensing layer consists of a 5 nm thick film of rubrene doped into TPD.

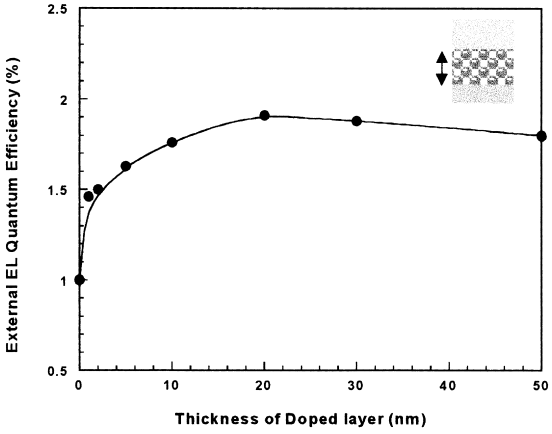

Fig. 9 External EL quantum efficiency as a function of thickness of the rubrene-doped TPD layer.

hole recombination occurs inside the Alq_3 layer, and leads to Alq_3 emission. A possible approach to eliminate this contribution and further improves the device efficiency is to block hole injection into Alq_3 by placing a thin film of a hole blocking material. In conclusion, electron-hole recombination on the highly fluorescent rubrene, maximized by the dual nature of rubrene acting as an electron hopping site and a hole trap in the host TPD, is proposed to be the dominant emission mechanism, and is largely responsible for the observed enhancement in electroluminescence quantum efficiency.

CONCLUDING REMARKS

Molecularly doped organic semiconductors, which exhibit very high fluorescence quantum yields in the solid state, have been developed at NRL. Absolute PL quantum efficiency close to unity has been achieved for some of these molecularly doped films. Förster dipole-dipole interaction between the guest

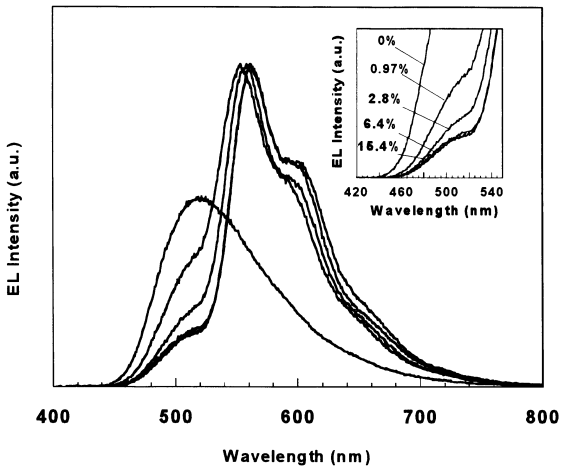

Fig. 10 EL spectra of rubrene: TPD as a function of rubrene concentration.

and the host molecules is proposed as the principal mechanism for efficient energy transfer with a rate of a nanosecond and a transfer range of 3–4 nm. These molecularly doped organic semiconductors were employed as the active emissive layers in molecular organic light-emitting diodes (MOLEDs). Devices based on multilayered structures using these active emissive layers were highly efficient. In metal quinolate-based devices where the active emissive layer consists of rubrene or DEQ doped into the metal quinolate, energy transfer from host to guest leads to the high EL quantum efficiency. A comparison between the absolute PL yield and the external EL efficiency suggests that the creation efficiency of the host excitons plays an important role in determining the maximum achievable EL quantum efficiency.

In devices where the active emissive layer consists of rubrene doped into the hole transporter TPD, direct carrier recombination on the highly fluorescent rubrene molecules is proposed to be the dominant EL mechanism. This is the result of the dual electronic nature of rubrene, which acts as an electron hopping site and a shallow hole trap in the host TPD.

ACKNOWLEDGEMENTS

Financial support from the Office of Naval Research (ONR) and the Defense Advanced Research Projects Agency (DARPA) is greatly appreciated.

REFERENCES

1 J. C. Scott, G. G. Malliaras. In *Conjugated Polymers* (G. Hadziioannou, P. F. van Hutten, eds). Wiley-VCH (1999).

2 T. Tsutsui. *MRS Bull.* **22**, 39 (1997), and references therein.

3 S. R. Forrest. *Chem. Rev.* **97**, 1793–1896 (1997), and references therein.

4 *Organic Electroluminescent Materials and Devices* (S. Miyata, S. Nalwa, eds). Gordon and Breach Science Publishers (1997).

5 *Organic Electroluminescence* (D. D. C. Bradley, T. Tsutsui, eds). Cambridge University Press (1996).

6 C. W. Tang. *Information Display* **12**, 16 (1996), and references therein.

7 N. C. Greenham, R. H. Friend. *Solid State Physics* **49**, 1–149 (1995), and references therein.

8 H. Murata, C. D. Merritt, Z. H. Kafafi. In *Science and Technology of Polymers and Advanced Materials*, pp. 207–214. Plenum Publishing Corporation, New York (1998).

9 H. Murata, C. D. Merritt, H. Mattoussi, Z. H. Kafafi. *Proc. SPIE*, **3476**, 88 (1998).

10 H. Murata, C. D. Merritt, Z. H. Kafafi. *IEEE J. of Select. Topics in Quantum Electronics* **4**, 119 (1998).

11 D. J. Fatemi, H. Murata, C. D. Merritt, Z. H. Kafafi. *Synth. Met.* **85**, 1225 (1997).

12 A. A. Shoustikov, Y. You, M. E. Thompson. *IEEE J. Select. Topics in Quantum Electronics* **4**, 3 (1998).

13 (a) T. Förster. *Fluorenzenz Organische Verbindungen*. Vandenhoech and Ruprech, Gottingen (1951); (b) T. Förster. *Discuss. Faraday Soc.* **27**, 7 (1959).

14 D. L. Dexter. *J. Chem. Phys.* **21**, 838 (1953).

15 H. Mattoussi, H. Murata, C. D. Merritt, Y. Iizumi, J. Kido, Z. H. Kafafi. *J. Appl. Phys.* **86**, 2642 (1999).

16 H. Mattoussi, H. Murata, C. D. Merritt, Z. H. Kafafi. *Proc. SPIE* **3476**, 49 (1998).

17 A. Dogariu, R. Gupta, A. Heeger, H. Wang, H. Murata, Z. H. Kafafi. *Proc. SPIE* **3797**, 38 (1999).

18 H. Murata, C. D. Merritt, Hiroshi Inada, Yasuhiko Shirota, Z. H. Kafafi. *Appl. Phys. Lett.* **75**, 3252 (1999).

19 G. Sakamoto, C. Adachi, T. Koyama, Y. Taniguchi, C. D. Merritt, H. Murata, Z. H. Kafafi. *Appl. Phys. Lett.* **75**, 766 (1999).

20 (a) J. Kido, Y. Iizumi. *Chem. Lett.* **963**, (1997); (b) ibid., *Appl. Phys. Lett.* **73**, 2721 (1998).

21 L. A. Crisafulli, H. Murata, C. D. Merritt, Z. H. Kafafi. *Proc. SPIE* **3797**, 432 (1999).

22 Y. Hamada, T. Sano. *Jpn. J. Appl. Phys.* **34**, L824 (1995).

23 H. Murata, H. Mattoussi, C. D. Merritt, Y. Iizumi, J. Kido, H. Tokuhisa, T. Tsutsui, Z. H. Kafafi. *Mol. Cryst. Liq. Cryst.* In press.